OPTIMIZATION OF SYSTEM OPERATION AND HEAT EXCHANGER SIZING IN RANKINE CYCLES: A CASE STUDY ON ALUMINIUM SMELTER HEAT-TO-POWER CONVERSION

Monika Nikolaisen[1]*, Trond Andresen[2]

SINTEF Energy Research, Gas Technology
Trondheim, Norway
Monika.Nikolaisen@sintef.no
Trond.Andresen@sintef.no

* Monika Nikolaisen

ABSTRACT

In industry processes worldwide, large amounts of heat in the temperature range 125-250 °C are rejected to the ambient. Utilization of this surplus heat for direct re-use or upgrading is the most efficient and cost-effective. However, lack of sufficient local heat demand can make heat-to-power conversion an attractive option for significant surplus heat utilization. Cost-effective heat-to-power conversion is challenging in the temperature range considered, and optimizing system design and operation is therefore important. This work describes optimization of heat exchanger sizing and system operation of an indirect Rankine cycle applied to heat-to-power conversion from aluminium smelter off-gas. The scenario involves a heat source with 850 kW heat duty available at a temperature of 150 °C. The overall system impact of considering heat source pressure loss was investigated in detail, as well as optimal distribution of heat transfer surface area between individual heat exchangers in the system. The system model is relatively detailed, including geometrically described heat exchangers discretized along the flow direction with local evaluations of fluid states, heat transfer coefficients and pressure gradients. The system was optimized with net power as objective function and by simultaneously optimizing process conditions and heat exchanger geometries. The total heat exchanger surface area was constrained to 750 m^2 during optimization. Results show that optimizing the system without accounting for the heat source pressure loss resulted in a net power production of 118 kW. Re-optimizing the system with a fan work penalty on pressure loss reduced net power by 21%. Optimizing heat transfer area distribution showed that the heat recovery heat exchanger should account for 68% of total heat exchanger area to maximize net power in a scenario with no penalty on heat source pressure loss. The fan work penalty on heat source pressure loss further increased heat recovery heat exchanger area requirement to 76% of total heat exchanger area.

1. INTRODUCTION

Analysis of Rankine cycles for surplus heat recovery is a widely researched topic typically motivated by the need to mitigate global warming through reduced energy use and emissions. Yang *et al.* (2015) performed such a study involving multi-objective optimization of a Rankine cycle for surplus heat recovery from engine exhaust gas. The study included detailed investigations of optimal Rankine cycle operation, but did not account for practical conditions such as heat exchanger pressure losses or power consumptions related to these. Nor did the study optimize sizing of individual heat exchangers. Kwak *et al.* (2014) performed a holistic analysis of integrating Rankine cycles for surplus heat recovery in a reference process industry based on a methodology named Total site analysis. The approach is targeted for analysis of site-wide energy efficiency and is less suited for investigating the effect of case specific conditions on optimum Rankine cycle performance.

Several articles have considered challenges specific to heat-to-power conversion in aluminium industry, where power can be produced by for instance utilizing the warm off-gas from aluminium smelters.

Aluminium smelters produce aluminium by high temperature electrolysis of alumina using significant electric input, with warm off-gases extracted from the smelters. Wang *et al.* (2012) analyzed the performance of Rankine cycles for power conversion from aluminium smelter off-gas. Their investigation focused on optimum evaporation temperature and working fluids for different heat source temperatures. The study did not involve optimization of operating conditions, or evaluation of heat exchanger sizes and overall system performance. Barzi *et al.* (2018) investigated the potential for power production using heat originating from side wall of aluminium electrolysis cells, and Ladam *et al.* (2014) evaluated the effect of lower heat source cooling limit on heat-to-power conversion from aluminium smelter off-gas. The latter study described several factors that make indirect Rankine cycles suitable for this application, including lower influence of the heat source cooling limit compared to direct Rankine cycles.

Yu *et al.* (2018) optimized the performance of a direct Rankine cycle for heat-to-power conversion from off-gas generated by aluminium production. The study accounted for the effect of heat source pressure loss on heat source fan power and net power production. However, the analysis was based on fixed heat source heat transfer coefficients and fixed heat source pressure loss, and neglected working fluid pressure losses and heat transfer performance. Moreover, geometry and sizing of individual heat exchangers was not optimized. The authors pointed out that the potential for power production is limited by low heat source temperatures, but claimed that power output could be increased using an "enhanced heat source" with less air dilution, yielding a heat source temperature of 150 °C for the evaluated case.

Few studies have been found that involve overall system optimization of indirect Rankine cycles applied to surplus heat recovery from aluminium smelter off-gas. Since this off-gas can be considered thermo-mechanically equivalent to air at ambient pressure, and with low pressure and volumetric energy content, heat source pressure loss is expected to have a high impact on system performance. Moreover, heat transfer from the off-gas to the Rankine cycle is limited by low heat source heat transfer coefficients, leading to a high heat transfer area requirement for the HRHE. The HRHE would in a practical application also be prone to particulate fouling on the off-gas side, causing further heat transfer resistance, but this is not accounted for in the current analysis. Instead, this study aims at evaluating the overall system impact of considering heat source pressure loss for a case study on power production from aluminium smelter off-gas, as well as the optimal distribution of heat transfer surface area between individual heat exchangers in the system. The methodology involves a "penalty" on heat source pressure loss in the form of fan work required to lift the heat source discharge pressure to its initial level, as well as optimization of both process conditions and heat exchanger geometries.

2. METHODOLOGY

2.1 Case description

The aluminium smelter off-gas case is described in Table 1 and Table 2, tabulating heat sink and heat source specifications, respectively. The case represents smelter off-gas at 150 °C collected from a cluster of cells in a hypothetical aluminium plant, constrained to a lower temperature limit of 80 °C. The heat source off-gas is modelled as air. The heat sink represents cooling water available at 10 °C, which a representative annual mean temperature in Scandinavia.

Table 1: Heat source specifications

Heat source	Unit	Value
Fluid	-	"Air equivalent"
Inlet temperature	(°C)	150
Lower limit outlet temp.	(°C)	80
Mass flow	(kg/s)	12
Pressure	(bar)	1

Table 2: Heat sink specifications

Heat sink	Unit	Value
Fluid	-	Water
Inlet temperature	(°C)	10
Mass flow	(kg/s)	23
Pressure	(bar)	5

2.2 Modelling and optimization

The modelled system is sketched in Figure 1; heat is recovered indirectly from the heat source through a heat recovery heat exchanger (HRHE) and indirect loop with pressurized water as heat transfer fluid. A heat source fan and indirect fluid pump provide power to the heat recovery process. The working fluid is propene, which receives heat from the indirect loop and produces power in an organic Rankine cycle. Excess heat is rejected to a water heat sink in the condenser, circulated with a heat sink pump. The heat sink pump is placed after the condenser to simplify modelling, but would be placed before the condenser in a practical application.

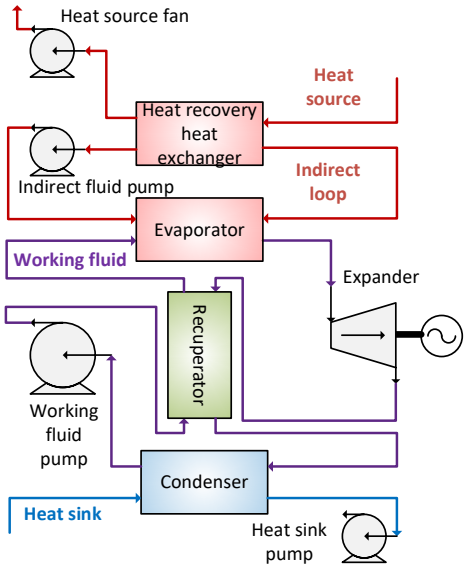

Figure 1: System sketch

The Rankine cycle is modelled and optimized using an approach named Generic heat exchanger analysis (Hagen *et al.*, 2019). Generic heat exchanger analysis involves maximizing net power based on simultaneous optimization of operating conditions and geometrically described heat exchangers. The heat exchangers are modelled as counter-current flow through channels on hot and cold sides, where the number of channels on both sides and tube length are optimized. Furthermore, the heat exchangers are discretized along the flow direction with local evaluations of fluid states, heat transfer coefficients and pressure gradients. The model used in this work resembles that described by Hagen *et al.* (2019), who modelled a direct Rankine cycle. However, the model has been adapted to an indirect cycle and a heat source fan has been included. Moreover, several additional condition- and geometry parameters can be optimized simultaneously, and higher relevance and quality of the results are expected. The modifications are described in Table 3; the reader is referred to Hagen *et al.* (2019) for a more detailed description of the methodology.

Table 3: Modifications of the analysis described by Hagen *et al.* (2019)

		Modified analysis	**Hagen *et al.* (2019) analysis**
Process model		Indirect Rankine cycle	Direct Rankine cycle
Geometry modelling and optimization	HRHE	Both sides	Working fluid side[1]
	Evaporator	Both sides	Not included
	Condenser	Working fluid side[2]	Working fluid side[2]
Process optimization	Working fluid and sink	Partly optimized[3]	Optimized
	Indirect fluid	Optimized	Not included
Calculation of heat exchanger surface area	HRHE and condenser	Hot and cold side average	Working fluid side
	Evaporator		Not included

[1]HRHE geometry on working fluid side was modelled and optimized, and heat transfer coefficient on source sides was fixed.
[2]In both models, heat sink heat transfer surface area was fixed to 100 m^2 to reduce the number of free variables.
[3]Condenser outlet pressure was fixed to 10 bar and heat sink mass flow to 23 kg/s to reduce the number of free variables.

The addition of full geometry description of the HRHE enables calculation of pressure loss on the heat source side. The equivalent fan work that this pressure loss corresponds to is calculated and included in the expression for net power output according to Equation 1.

$$\dot{W}_{net} = \dot{W}_{expander} - \dot{W}_{wf\ pump} - \dot{W}_{sink\ pump} - \dot{W}_{indirect\ pump} - \theta \cdot \dot{W}_{source\ fan} \quad (1)$$

where θ is a "fan work weight factor" between 0 and 1.

The fan work weight factor enables analysis of how the system re-optimizes when accounting for the heat source pressure loss to a varying degree. It can be argued that it would be unbalanced to subtract 100% of the calculated fan work in the expression for net power in this context, due to where the system

boundaries for the analysis are set, shown in Figure 2. In an actual industrial application of heat recovery from off-gas, the cooling of the heat source would cause lower-than-nominal pressure loss and fan work downstream of the HRHE, or energy recovery unit (ER), owing to a higher density and thus lower volume flow rate. In the case of an aluminium smelter, pressure loss from the gas treatment center (GTC) inlet to the exhaust stack is typically in the range of several thousand pascals. Even a fractional reduction in nominal pressure loss in the GTC will be significant compared to expected HRHE pressure loss. Consequently, even though the additional pressure loss in the HRHE is real and causes a fan work penalty, the change in net system fan work will be less than 100% $\cdot \dot{W}_{source\ fan}$. The impact on net system fan work is not possible to determine without extending system boundary and considering a detailed aluminium plant. To obtain results that could be valid on a general basis, the analysis is performed for variable fan work weight factors.

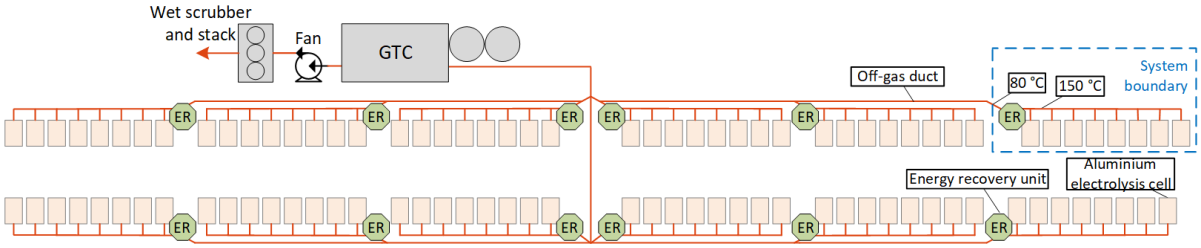

Figure 2: Conceptual sketch of power production from off-gas in an aluminium plant; the system boundary only covers one energy recovery unit and off-gas collected from a cluster of eight aluminium cells.

Calculation of heat exchanger surface areas has been modified compared to the original generic heat exchanger approach, as shown in Table 3. Since heat exchangers in this work are geometrically described on both hot and cold sides, heat exchanger areas can be calculated as the hot and cold side average. Heat exchangers in the original generic heat exchanger approach were only geometrically described on the working fluid sides, and thus heat exchanger area could only be represented by the area on the working fluid side. Calculation of recuperator area has not changed. In the absence of in-depth economic functions per component, the sum of all heat exchanger areas could be considered as an initial representation of system costs. At initial design stages, it is not obvious whether the hot or cold side of the heat exchangers have the highest cost, and therefore the average is used in the calculation of total area. Furthermore, cycle optimization involves maximizing net power, Equation 1, with a constraint on the total heat exchanger area. Free optimization variables and optimization constraints are given in Table 4 and Table 5, and fixed parameters are given in Table 6. REPROP 9 was used for calculating thermodynamic properties, and the system was optimized with the gradient-based constrained optimisation solver NLPQL (Schittkowski, 1986). Heat transfer and pressure loss correlations are given in Table 7.

Table 4: Free optimization variables

Working fluid and indirect fluid mass flow
Expander inlet enthalpy and pressure
HRHE cold side inlet temperature
Heat exchanger lengths
Heat exchanger number of channels, both sides[1]

[1]Condenser cold side number of channels is fixed to 32 to yield a heat transfer surface area of 100 m^2.

Table 5: Optimization constraints

Constraint	**Unit**	**Value**
Minimum heat source outlet temperature	(°C)	80
Total heat exchanger surface area[1]	(m^2)	750
Fan work weight factor, θ[2]	-	0, 0.25, 0.50, 0.75 and 1

[1]An area of 750 m^2 was set to represent a relatively large system with small temperature differences, utilizing most of the available potential in the heat source

[2]A total of five optimizations are performed, each with a different fan work weight factor as listed.

Table 6: Fixed parameters

	Parameter	Unit	Value
Pumps	Isentropic efficiency	-	0.70
	Motor efficiency	-	0.95
Expander	Isentropic efficiency	-	0.85
	Generator efficiency	-	0.95
Fan	Isentropic efficiency	-	0.90
	Motor efficiency	-	0.95
HRHE	Hydraulic diameter, indirect fluid side	(mm)	10
	Hydraulic diameter, source side	(mm)	60
Evaporator	Hydraulic diameter, working-fluid side	(mm)	10
	Hydraulic diameter, indirect fluid side	(mm)	20
Condenser	Hydraulic diameter, working-fluid side	(mm)	20
	Hydraulic diameter, sink side	(mm)	20
	Sink side cross sectional area	(cm^2)	100
Recuperator	Hydraulic diameter, low-pressure side	(mm)	20
	Hydraulic diameter, high-pressure side	(mm)	10
Fluids	Working fluid	-	Propene
	Indirect fluid	-	Water

Table 7: Heat transfer and pressure drop correlations employed in the model

Flow	Heat transfer	Pressure drop
Single-phase	Gnielinski (1976)	Selander (Selander, 1978)
Two-phase	Boyko and Kruzhilin (1967) (condensation)	Friedel (1979) with single-phase formulation by Selander (1978)

3. RESULTS AND DISCUSSION

A total of five system optimizations have been performed, each with a different fan work weight factor according to Table 5. In this section, results originating from these optimizations are presented with fan work weight factor on the x-axis. This presentation demonstrates how results for optimized system parameters vary with increasing fan work penalty on heat source pressure loss. Figure 2 shows the main results from cycle optimization, i.e. variation in expander power, pumping and fan power, and net power with increasing fan work weight factor. With increasing fan weight, expander power decreases and power consumptions go up, yielding a reduction in net power from 118 kW to 93 kW (-21%).

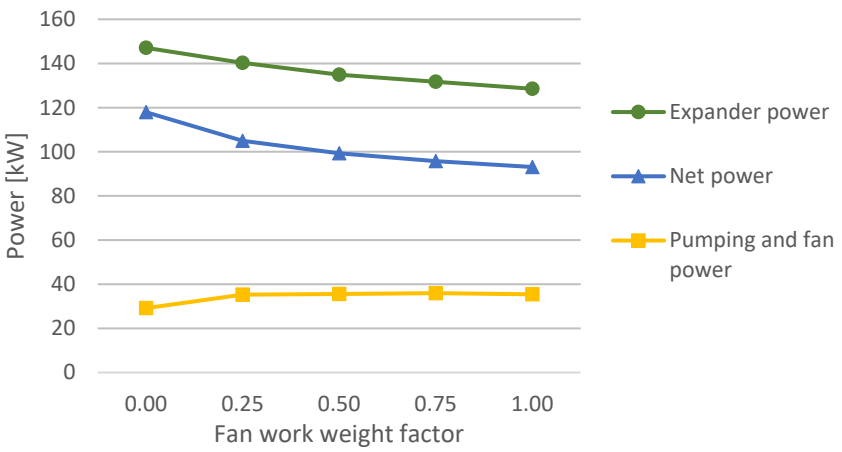

Figure 3: Development in expander power, pumping and fan power, and net power with fan work weight factor

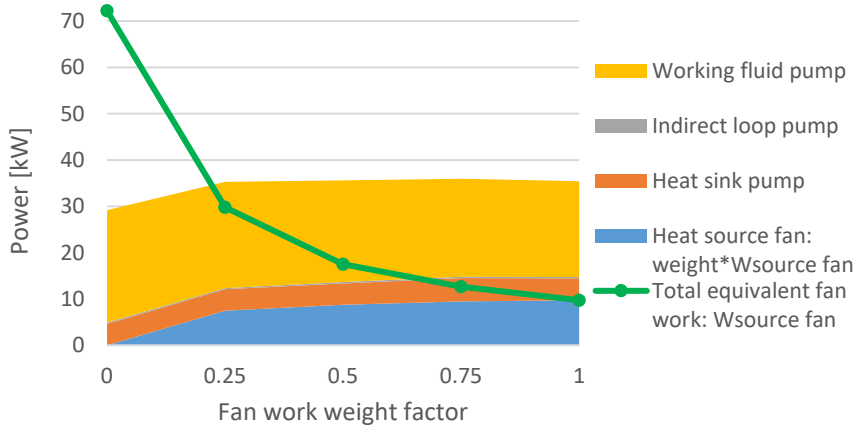

Figure 4: Development in pumping and fan work with fan work weight factor

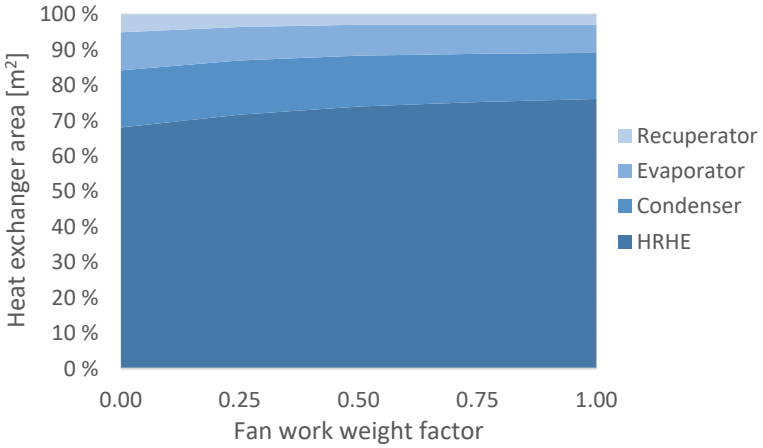

Figure 5: Optimized distribution of individual heat exchanger areas with fan work weight factor

Figure 3 shows the individual pumping and fan power consumptions, as well as the total equivalent heat source fan work, $W_{source\ fan}$ (green line). Note that only the value of $\theta \cdot W_{source\ fan}$ (blue area) is accounted for in the net power, as opposed to the total equivalent fan work. Clearly, the total equivalent fan work becomes high when it is not optimized (i.e. not included in the net power, $\theta = 0$), reaching a value of 72 kW for a maximum heat source pressure loss of 5 kPa. The total equivalent fan work is more than half the net power in this case, but the optimizer is able to reduce this value to 10 kW when the total fan work is included in the net power ($\theta = 1$). Thus, the value of $\theta \cdot W_{source\ fan}$ increases with fan weight, but flattens out since the optimization is able to reduce the total equivalent fan work, $W_{source\ fan}$ by finding a better overall system design.

Figure 4 shows the optimized percentage distribution of total heat exchanger area with varying fan work weight factor. Recall that the total heat exchanger area is the same for all five cases, meaning that percentage changes will reflect absolute changes in area. The HRHE is obviously the largest heat exchanger, and accounts for roughly 70% of total area in most cases. As more of the total equivalent fan work is accounted for in the net power, the fraction of HRHE area increases (from 68 % to 76 % going from 0 to 1 fan work weight factor), causing the other heat exchangers to become smaller due to the constraint on total heat exchanger area of 750 m^2.

Figure 5 and Figure 6 plot the change in key performance parameters of the HRHE with increasing fan work weight factor. Figure 5 shows the change in optimized pressure loss and number of channels on the heat source side. When heat source pressure loss is penalized with fan work (increasing fan work

weight factor), heat source pressure loss reduces, enabled by a higher number of channels (and shorter channels, which is not shown in the figure).

Figure 6 shows the individual factors contributing to the HRHE heat balance given by Equation 2, which calculates the HRHE heat duty as a multiple of the overall heat transfer coefficient, U, hot and cold side average heat transfer area, $A_{average}$, and the mean temperature difference, ΔT:

$$\dot{Q}_{HRHE} = UA_{average}\Delta T \quad (2)$$

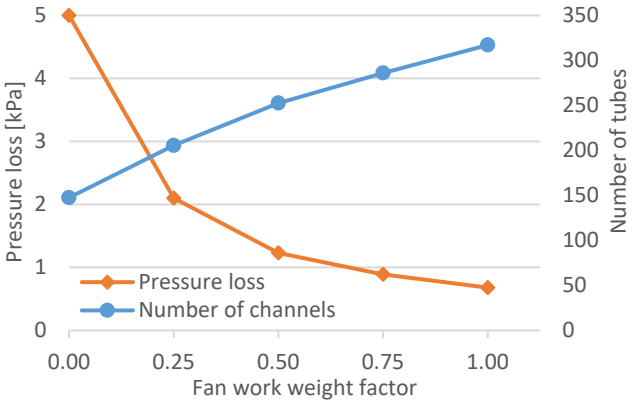

Figure 6: Change in HRHE pressure loss and number of channels on heat source side with fan work weight factor

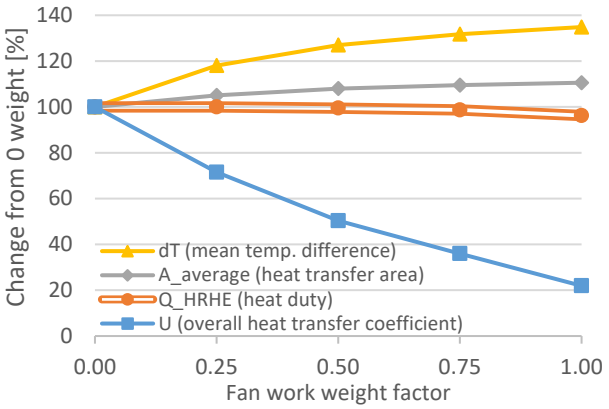

Figure 7: Change in HRHE heat duty, heat transfer coefficient, heat exchanger area and average temperature difference with fan work weight factor

Figure 6 demonstrates that the heat transfer coefficient is significantly reduced with fan work weight factor, owing to the reduction in pressure loss. Lower heat transfer coefficient is compensated by a higher temperature approach and a higher area. However, the reduction in heat transfer coefficient dominates, causing a slight reduction in heat duty with increasing fan work weight factor. The result of a higher temperature approach and lower duty in the HRHE is a decrease in HRHE performance and thus expander power. Owing to the constraint on total heat exchanger area of 750 m^2, a higher HRHE area also corresponds to lower condenser, evaporator and recuperator areas, causing higher exergy loss in these, and consequently lower expander power.

From Figure 2 it is obvious that net power decreases when penalized by the equivalent fan work from heat source pressure loss. The penalty for each weight factor above 0 is a combination of fan work, lower HRHE performance and higher exergy destruction in the other heat exchangers. However, overall system re-optimization for each evaluated case ensures a best possible compromise within the given conditions and constraints; from 0 to 1 fan work weight factor, optimization yields a reduction in total equivalent fan power of 87% and a comparatively low compromise in net power of -21%.

5. CONCLUSIONS

This work has provided insight into optimum design of an overall system for power production from aluminium smelter off-gas. The effect of heat source pressure loss was investigated by calculating the fan work corresponding to the heat source heat exchanger pressure loss. System optimization showed that the heat source pressure loss can be fully accounted for with a compromise in net power of -21%. Moreover, system optimization strongly favors a large heat recovery heat exchanger, which should account for 68% of total heat exchanger area to maximize net power in a scenario with no penalty on heat source pressure loss. The large heat recovery heat exchanger area requirement is caused by poor heat transfer performance on the gas side of the heat exchanger. The fan work penalty on heat source pressure loss further increased heat recovery heat exchanger area requirement to 76% of total heat

exchanger area. Overall system optimization proves to be a powerful tool for optimizing overall system performance when the system is constrained by practical conditions such as heat source fan power.

NOMENCLATURE

A	heat transfer surface area	(m^2)
av	average	(-)
HRHE	heat recovery heat exchanger	(-)
$\dot{Q}$	heat duty	(W)
U	overall heat transfer coefficient	(W/m^2K)
$\dot{W}$	power	(kW)
temp	temperature	(K)
ΔT	temperature difference	(K)
θ	fan work weight factor	(-)

Subscript

sink	heat sink
source	heat source
wf	working fluid

REFERENCES

BARZI, Y. M., ASSADI, M. & PARHAM, K. 2018. A waste heat recovery system development and analysis using ORC for the energy efficiency improvement in aluminium electrolysis cells. *International Journal of Energy Research,* vol. 42**,** p. 1511-1523.

BOYKO, L. D. & KRUZHILIN, G. N. 1967. Heat transfer and hydraulic resistance during condensation of steam in a horizontal tube and in a bundle of tubes. *International Journal of Heat and Mass Transfer,* vol. 10**,** p. 361-373.

FRIEDEL, L. 1979. *Improved Friction Pressure Drop Correlations for Horizontal and Vertical Two-Phase Pipe Flow*.

GNIELINSKI, V. 1976. New Equations for Heat and Mass Transfer in Turbulent Pipe and Channel Flow. vol. 16**,** p. 359-368.

HAGEN, B., NIKOLAISEN, M. & ANDRESEN, T. 2019. A novel methodology for Rankine cycle analysis with generic heat exchanger models *In review process with the journal Applied Thermal Engineering,* vol. -.

KWAK, D.-H., BINNS, M. & KIM, J.-K. 2014. Integrated design and optimization of technologies for utilizing low grade heat in process industries. *Applied Energy,* vol. 131**,** p. 307-322.

LADAM, Y., BØRGUND, M. & NÆSS, E. Influence of heat source cooling limitation on ORC system layout and working fluid selection: The case og aluminium industry. TMS Light Metals, 2014. 723-727.

SCHITTKOWSKI, K. 1986. NLPQL: A fortran subroutine solving constrained nonlinear programming problems. *Annals of Operations Research,* vol. 5**,** p. 485-500.

SELANDER, W. N. 1978. Explicit formulas for the computation of friction factors in turbulent pipe flow. Chalk River, Ontario, Canada: Chalk River Nuclear Labs.

WANG, Z., ZHOU, N. & JING, G. 2012. Performance analysis of ORC power generation system with low-temperature waste heat of aluminum reduction cell. *Physics Procedia,* vol. 24**,** p. 546-553.

YANG, F., ZHANG, H., SONG, S., BEI, C., WANG, H. & WANG, E. 2015. Thermoeconomic multi-objective optimization of an organic Rankine cycle for exhaust waste heat recovery of a diesel engine. *Energy,* vol. 93**,** p. 2208-2228.

YU, M., GUDJONSDOTTIR, M. S., VALDIMARSSON, P. & SAEVARSDOTTIR, G. 2018. Waste heat recovery from aluminum production. *Minerals, Metals and Materials Series.*

ACKNOWLEDGEMENT

The authors gratefully acknowledge the financial support from the Research Council of Norway (EnergiX grant no. 255016/E20) for the COPRO project, and the user partners Equinor, Hydro, Alcoa, GE Power Norway and FrioNordica.